A METHODOLOGY FOR MEASURING THE VELOCITY AND THICKNESS OF WAVE-INDUCED UP-RUSHING JETS ON VERTICAL SEAWALLS AND SUPERSTRUCTURE

Gholamreza Shiravani[1], Michalis Vousdoukas[2], Stefan Schimmels[3] and Dimitris Stagonas[4]

Waves breaking on vertical seawalls result in up-rushing water jets with high velocities, which in turn lead to large overtopping rates and pose a serious threat to pedestrians, vehicles or any infrastructure in the vicinity of the seawall. Nevertheless, knowledge on the characteristics, namely the velocity and thickness, of such jets is scarce. Based upon recent experiments in the Large Wave Flume (Großer Wellenkanal, GWK) of Forschungszentrum Küste (FZK) the current paper proposes a semi-automated methodology for measuring velocity and thickness of up-rushing jets. The methodology was applied on cases considering waves ranging from non-breaking to nearly and strongly breaking and yielded encouraging results. With regards to the velocities a good repeatability is reported for non-breaking waves, while for breaking waves velocities are, as anticipated, observed to depend on the intensity of breaking. When the thickness is concerned, user based decisions are required as the selection process is drastically affected by the increased air content of the up-rushing jet.

Keywords: vertical seawall; recurve/parapet; breaking waves; up-rushing jet velocity

1 Introduction

Vertical seawalls constitute coastal structures typically installed along coastlines to protect the landward areas against the incoming waves. However, recent changes in extreme wave climate and water levels apply additional pressure on existing seawalls (Burcharth et al., 2014). It is noteworthy that after the recent winter storms in the UK, the Association of British Insurance (ABI) announced insurance claims related to flood damages, reaching 6.7 £ per day (www.abi.org.uk). Furthermore, the mortality rate due to overtopping or falling from the coastal barriers is unfortunately estimated to two to four persons per year in the UK (Allsop et al., 2005). To address these challenges more efficient coastal protection designs are necessary towards that direction, parapets or wave recurve/bullnose could substantially reduce the overtopping rate and consequently increase the safety of protected infrastructures and individuals.

In order to efficiently design such super-structures knowledge on the characteristics of the water-jet interacting with them is required; see for example Figure 1. As cited in Allsop et al. (2005) and Wolters et al. (2005), de Rouville et al. (1938) reported field measurements of up-rushing jet velocities up to 77 ms^{-1} or about 7 times the horizontal velocity of the wave. Nevertheless, the extent of available data sets on the up-rushing velocities of wave induced jets is rather low. Bruce et al. (2002) and Wolters et al. (2005) provided measurements of throw/up-rushing velocities for both small and large scale but their acquisition and processing approach was labor intensive and at occasions uncertain; the former authors manually analyzed low-speed VHS records while the latter extracted velocity estimations from records collected by a small number of pressure sensors and pressure aeration units.

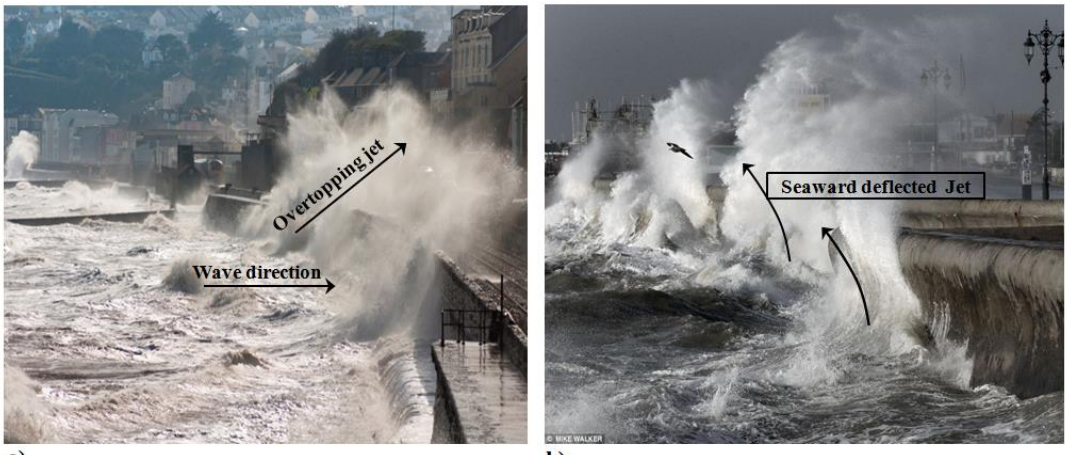

Figure 1. Water waves hitting a seawall during recent storms in the UK; a) without recurved crown and b) deflected waves from recurved crown.

[1] Forschungszentrum Küste (FZK), Merkurstr. 11, 30419, Hannover, Germany, shiravani@fzk-nth.de
[2] Joint European Research Center, Institute of Environment and Sustainability, Via Enrico Fermi 2749, I-21027-Ispra, Italy, michalis.vousdoukas@jrc.ec.europa.eu
[3] Forschungszentrum Küste (FZK), Merkurstr. 11, 30419, Hannover, Germany, schimmels@fzk-nth.de
[4] Civil, Environmental and Geomatic Eng., University College London, WC1E 6BT, London, UK, d.stagonas@ucl.ac.uk

The current work, presents a semi-automated methodology to measure water-jet velocities recorded by a high speed camera at any point on a vertical seawall. The methodology is tested with water-jets induced by regular non-breaking and breaking waves and velocities are measured at different locations on the seawall. Results are accordingly used to assess its performance. In addition, it is shown that by locating the camera within the flume and by placing very thin, seawards protruding elements at the edge of the wall, the simultaneous measurement of water-jet velocity and water-jet thickness is possible. To the best of our knowledge this is the first time that velocity measurements are complemented with information on the thickness of the up-rushing water-jet.

2 Methods

2.1 Experimental model-setup

The reported experiments in GWK were part of a Translational Access project within Hydralab IV (www.hydralab.eu) performed in summer 2012. An overview of the experimental set-up is shown in Figure 2.

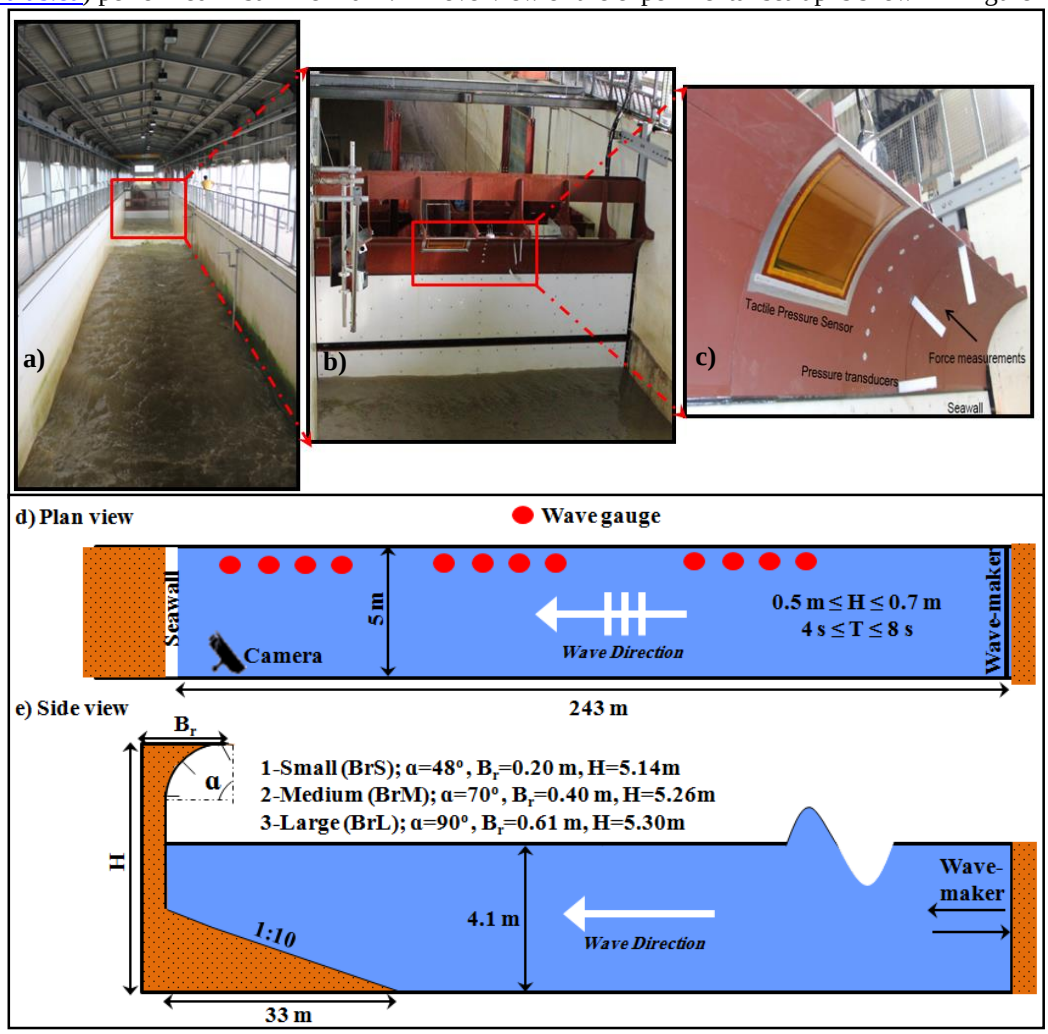

Figure 2. Experimental model set-up: a) GWK and retrofitted seawall exposed to water waves, b) instrumented seawall and recurve, c) equipped recurve with blades and pressure sensors, d) plan view and e) side view of the experimental set-up.

A vertical seawall with a circular shaped wave recurve on top was installed 241m off the wave-maker and in front of the structure a 33 m long 1:10 slope was placed in order to induce wave breaking. Waves were measured along the flume by 12 resistance type wire wave gauges arranged in arrays to allow for reflection analysis. The wall was equipped with standard pressure and force transducers as well as a special tactile pressure sensor in order to determine the total load and the load distribution on the superstructure. However, the present paper does not deal with the loads directly but rather with their cause by the up-rushing water jets, which were recorded at 300 frames

per second (fps) with a high speed video camera installed inside the flume about 1 m above still water level. In order to determine the water-jet thickness, 15 mm thick and 28 cm long blades were mounted at the underside of the recurve.

Actually three different recurves with 48°, 70° and 90° opening angle were investigated, but in the following only the medium case with 70° will be considered exemplarily for the further presentation of the applied methodology and the discussion of the results.

2.2 Image processing

The applied methodology consists of 5 steps for non-intrusive measurements of the jet position/velocity on the seawall and simultaneous measurements of the jet layer thickness based on image processing of the video data from the high speed camera. An overview of the first two steps is shown in Figure 3.

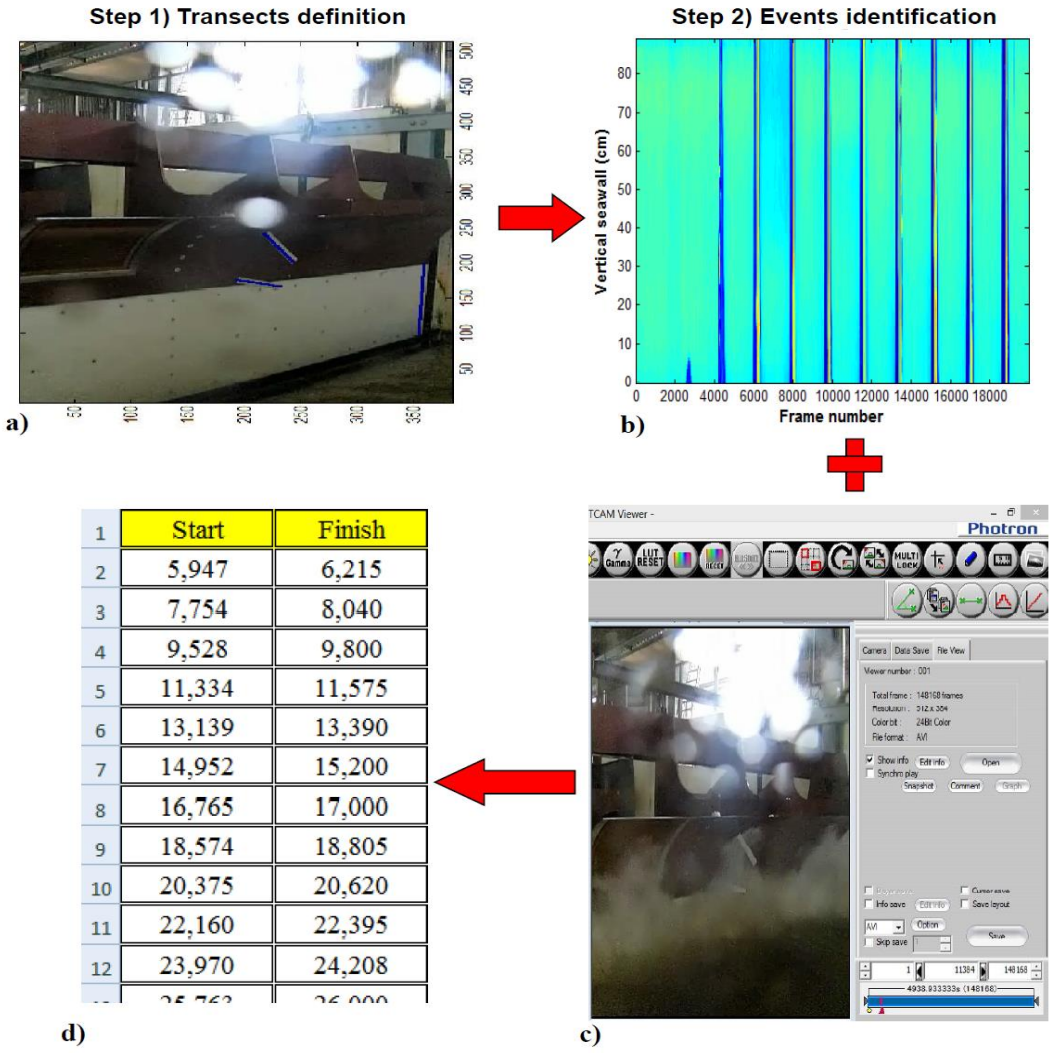

	Start	Finish
2	5,947	6,215
3	7,754	8,040
4	9,528	9,800
5	11,334	11,575
6	13,139	13,390
7	14,952	15,200
8	16,765	17,000
9	18,574	18,805
10	20,375	20,620
11	22,160	22,395
12	23,970	24,208

Figure 3. Steps 1 and 2 – Identifying wave events; a) vertical seawall and selected transects (blue lines), b) time-stack image of one transect on the seawall, c) event visualization using Photron FASTCAM viewer and d) table of events start and end.

Step1: Defining the measuring transects

The video analysis was based on time-stack images which are a standard approach to trace wave fronts along the surf and swash zone (e.g. Aagaard and Holm, 1989; Catalan and Haller, 2008; Vousdoukas et al., 2014; Vousdoukas et al., 2012b; Vousdoukas et al., 2009). For the present case (i) three vertical sampling transects were defined along the seawall to track up-rush motions and (ii) additional transects were considered along each of the blades in order to track the jet thickness (blue lines in Figure 3a).

Step2: Identifying the wave up-rush events

An event is defined as an interval of a recorded video in which a wave hits the seawall and is returned by the recurve seawards, i.e. each individual test/video constitutes of several events. The first step to analyze a recorded video is identifying the initial and final frames of each event by (i) defining a transect on the seawall; (ii) generating a time-stack image by sampling the pixel intensities along the transect (Figure 3b); (iii) identifying the up-rush events from the temporal pixel intensity variations (dark blue areas in Figure 3b) and (iv) confirming the event incidence through visual inspection of the actual video frames. Time stack analysis was done in Matlab© while for the visual inspection of the high speed camera videos the Photron FASTCAM viewer software (Figure 3c) was used.

Step3: Pixel intensity sampling and time-stack image enhancement

Instead of generating the time-stack images from the original images the frames were enhanced by subtracting the intensity values of each image (Figure 4b) with the intensities of a reference image with calm water surface (Figure 4a). This approach results in a more pronounced jet-tip (Figure 4c) allowing for a more robust feature tracking as described in step 5 below. Furthermore, the thin jet layer at the leading edge can be distinguished much better from the water mass of the actual wave (dark water in the raw image, Figure 4b).

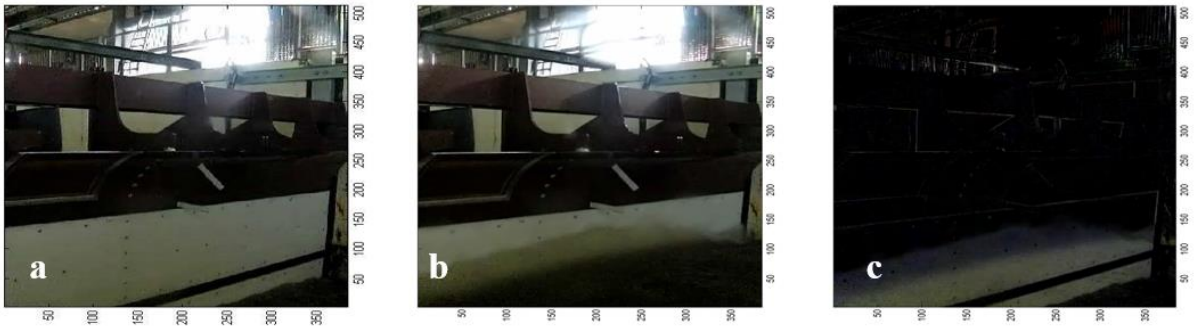

Figure 4. Image enhancement example: a) reference image, b) raw image with up-rushing jet, c) difference image.

Step4: Coordinate transformation

The jet up-rush position was initially obtained in pixel coordinates and transformation to metric coordinates took place using standard photogrammetric techniques, considering lens distortion and camera geometry (Vousdoukas et al., 2012). For the time-stack images generated in the present application the pixel footprint was around 0.2 cm and 0.1 cm in vertical and horizontal direction, respectively, resulting in a total measurement error after both coordinate transformation and feature detection, which was always below 0.5 cm with an average value of 0.33 cm.

Step5: Jet-interface tracking

After the time stack images have been transformed to metric coordinates they can be used to determine the jet velocity and layer thickness either by visual inspection or by automatic detection based on pixel intensities. Figure 5 exemplarily shows three timestack images based on difference images (a – c) and on raw images (f – h). The edge of the jet can be immediately interpreted visually by the sudden change in pixel intensity and the result of such a visual inspection is shown by the black lines in Figure 5 (f – h). However, it can also be seen that the interface in the raw image time stacks is more blurred than in those based on the difference images, which becomes more obvious from the detailed sections in Figure 5d and e. Therefore an automatic detection of the edge using a simple threshold value for the pixel intensities will only provide useful outcomes for the difference time stacks. Corresponding results are marked by the black lines in Figure 5 (a – c), which apart from some fluctuations suggest a more or less linear increase of jet position and layer thickness, i.e. a constant jet velocity and layer thickness growth rate. The red lines confirm the linear trend as they are based on the average jet velocity and thickness growth rate.

Several tests have been analyzed with the automatic detection and always the same trend could be observed. In the following the validity of the applied method will be discussed based on exemplary results of the jet velocity.

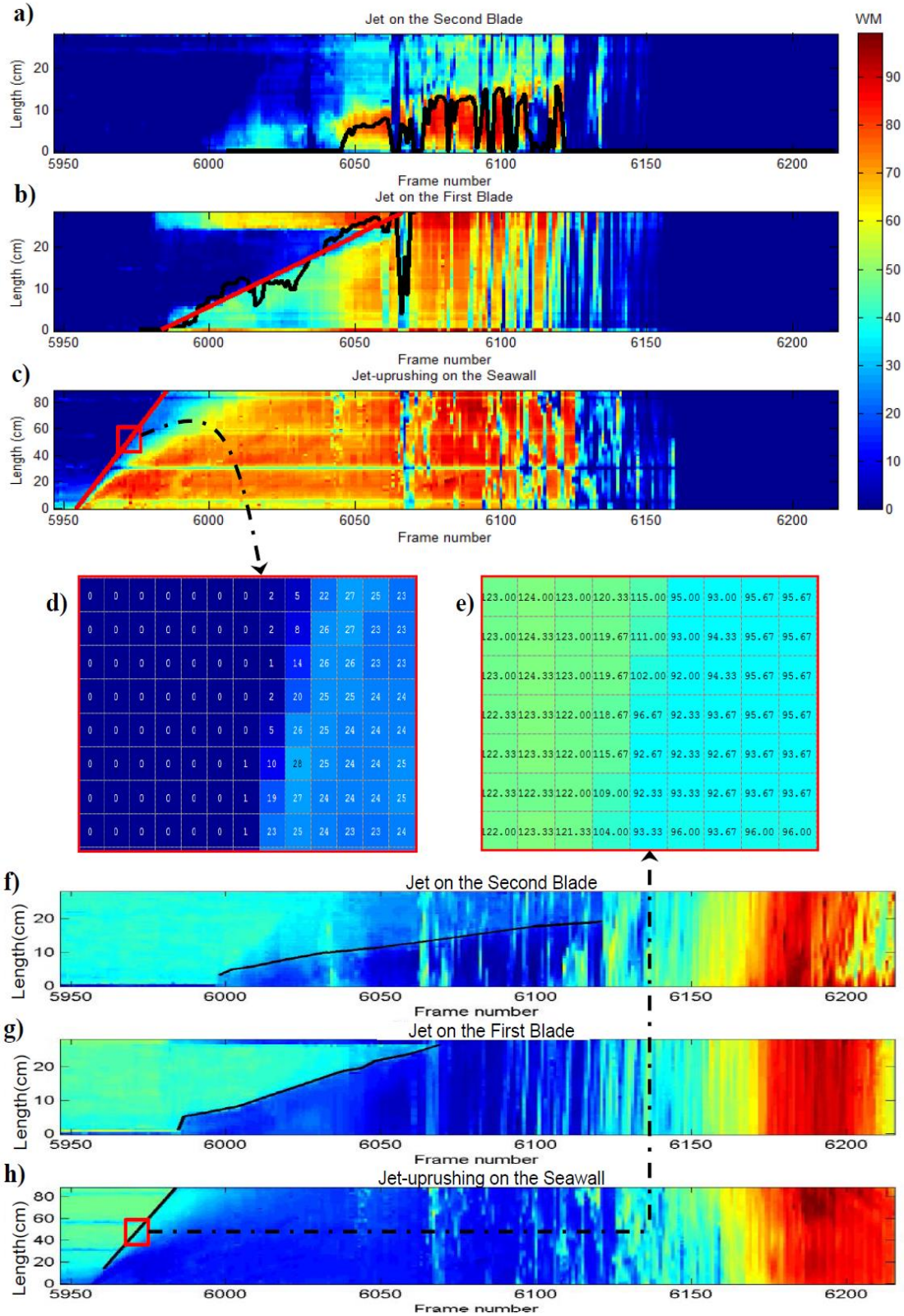

Figure 5. Comparison of feature tracking on enhanced (a-d) and standard timestack images (e-h): Three time-stack images are shown for each case for the upper (a, f) and lower blade (b, g) and for the seawall (c, h), while d and e zoom on the pixel intensity variations at the feature edges. Black and red lines indicate the feature tracking result.

3 Results and discussion

Since a similar data set for comparison, is not available in the existing literature and in order to reassure the quality of the data several randomly selected cases of the automatic tracking results were cross-referenced with visual inspection of the video frames. In a similar manner to the example shown in Figure 6 a good correlation was always observed as the jet trace extracted from the processed image(s) (red dots in Figure 6) was found to overlap with the one on the video frames.

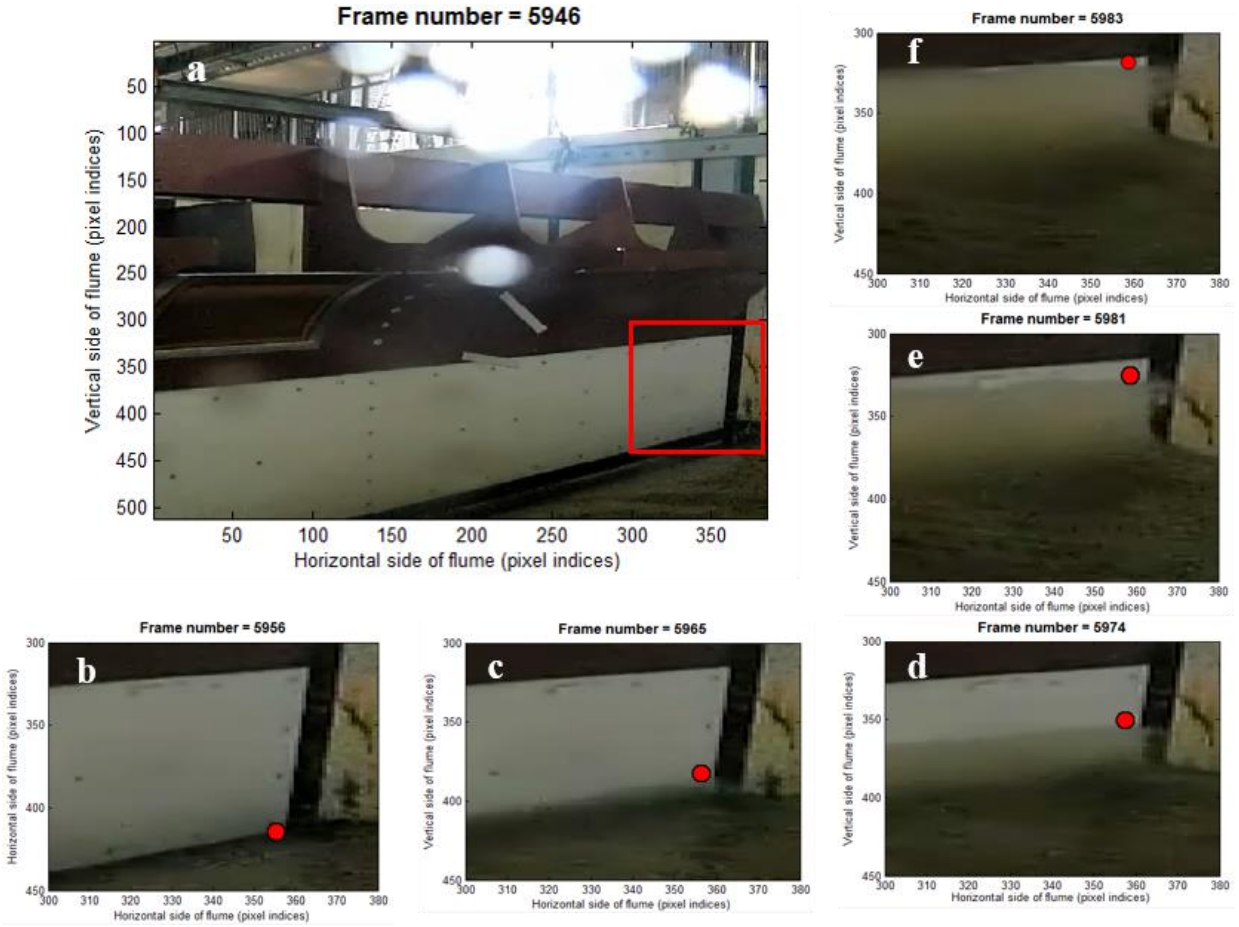

Figure 6. Validation of the automatic image analysis results by visual comparison of image frames: a) Image of the seawall before the wave event; b) event initiation; c) jet formation, e-f) jet evolution. Red square in panel a) marks the displayed area in panels b) – f) where the red circles indicate the jet position determined from the image processing technique.

The suggested methodology was applied to both non/nearly-breaking and breaking waves. As the tip of the crest/jet rushes up the wall, a record of its displacement over time is produced. The steepness of the line connecting two subsequent displacement points is of course the speed of the tip at that moment in time, $u_z(t)$. For the maximum tip-speed calculated for events occurring under the same incoming wave conditions a non-negligible scatter on the data was observed. This is hardly surprising as within the small time intervals (3.3ms) between each frame and especially near the impact zone $u_z(t)$ is strongly dependent on the local conditions. Nevertheless, and assuming that the methodology does not underperform, velocity fluctuations between subsequent events should reduce if $u_z(t)$ is averaged over the recording time for each analysed event.

In Figure 7 this average jet velocity is plotted over the number of subsequent events for a non-breaking, a nearly/weakly breaking and a strongly breaking wave. Indeed, for the non-breaking wave (Figure 7a) the scatter in the averaged crest/jet velocity is negligible and it gradually increases as the intensity of breaking increases. It is noteworthy that the first waves arriving at the wall are either underdeveloped and below the breaking limit resulting in smaller velocities (Figure 7b) or they break under cleaner conditions and thus they result in faster water-jets (Figure 7c).

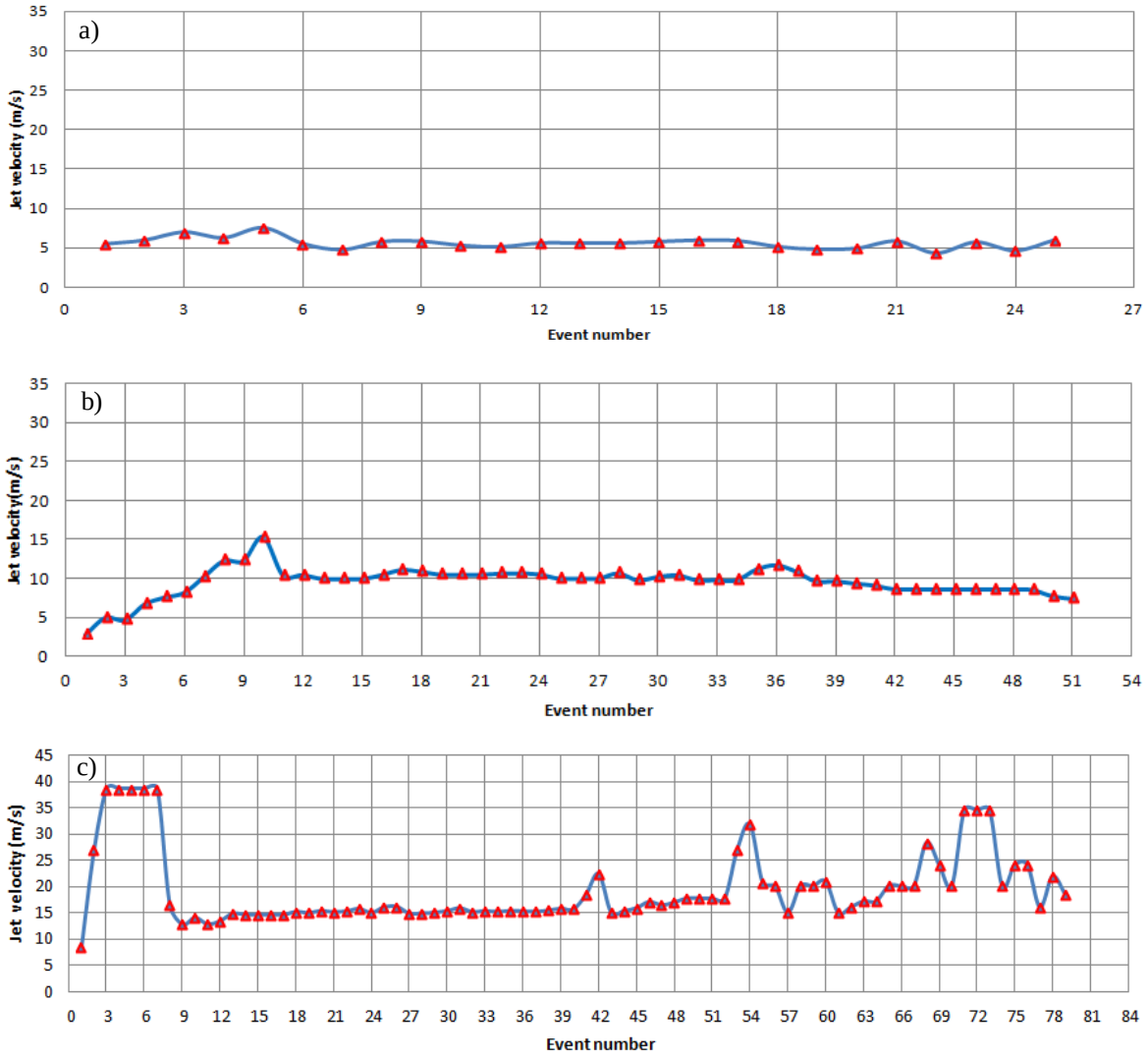

Figure 7. Evolution of averaged up-rushing jet velocities for a) a non-breaking, b) a nearly/weakly breaking and c) a strongly breaking wave case.

The capacity of the methodology was also assessed by comparing results at three different transects along the wall (Figure 8a). Figure 8 (b – d) shows the temporal evolution of the average jet velocity and Figure 9 the correlation between the results at the different locations. The results at section C5 and C9 correlate quite well while C1 shows reduced velocities, most probably due toto wall effects. A comparison of Figure 7c and Figure 8 also supports the current methodology, as breaking waves with the same period (T = 6 s) but larger height (H = 0.7 m for Figure 7c and H = 0.6 m for Figure 8) consistently result in faster water-jets.

It is noteworthy that maximum up-rush velocities measured for breaking induced jets ranged between 10-13 times the shallow water velocity. This compares fairly well with Bruce et al. (2002), who measured factors up to 11 and up to about 6 for large and small scale tests, respectively, and Wolters et al. (2005) who also reported similar values for tests conducted in GWK.

Despite the methodology's encouraging performance for water-jet velocity measurements, acquiring information about the thickness of the jet is more difficult since the high air content and the decomposition of the jet into droplets obscure the view on the blade (cf. Figure 4c) Therefore user based decisions are still required.

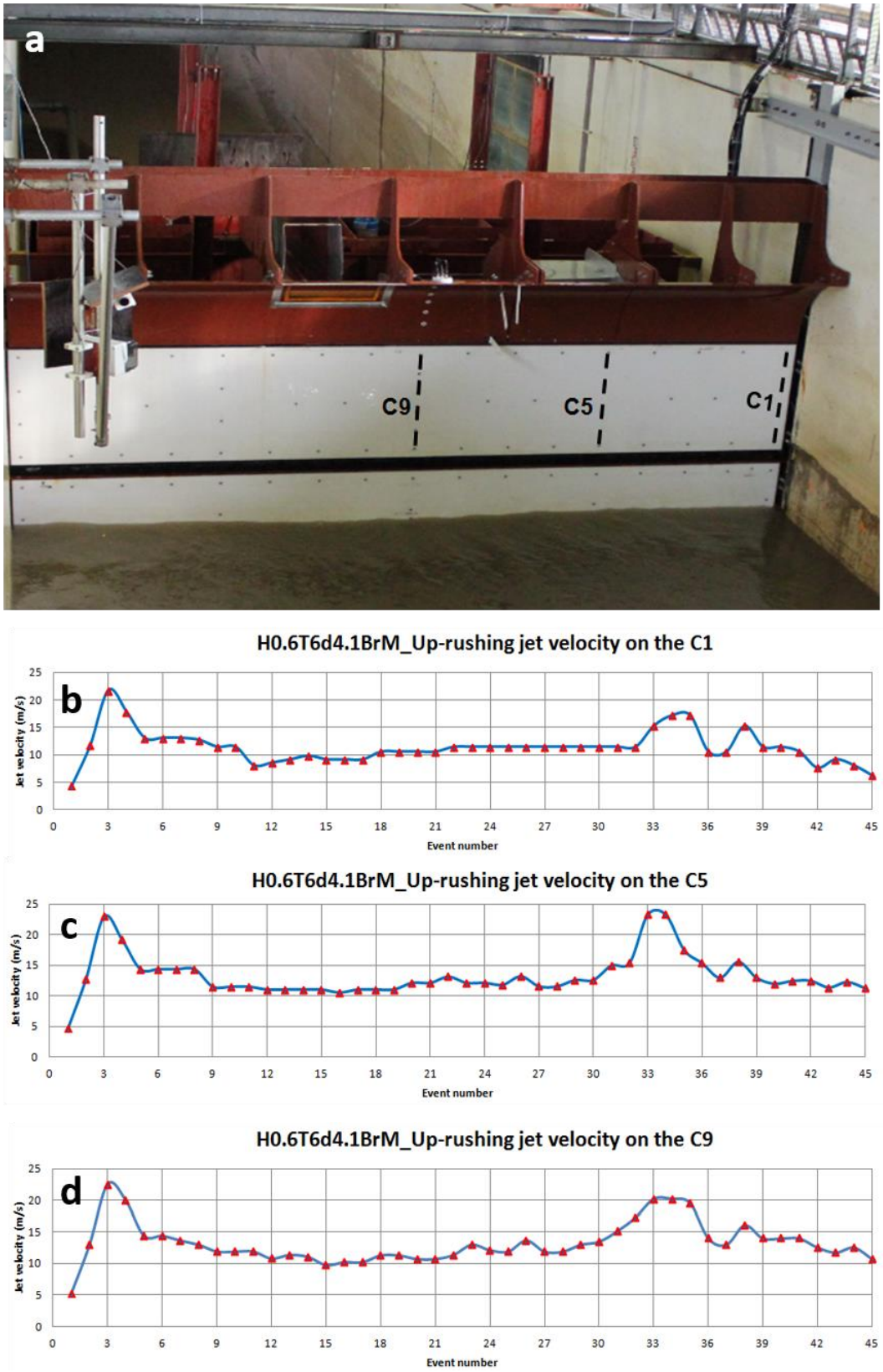

Figure 8. Evolution of jet velocity at three different transects along the wall. a) Seawall with selected transects (dashed black lines); b) jet velocity at transect C1; c) jet velocity at transect C5; d) jet velocity at transect C9.

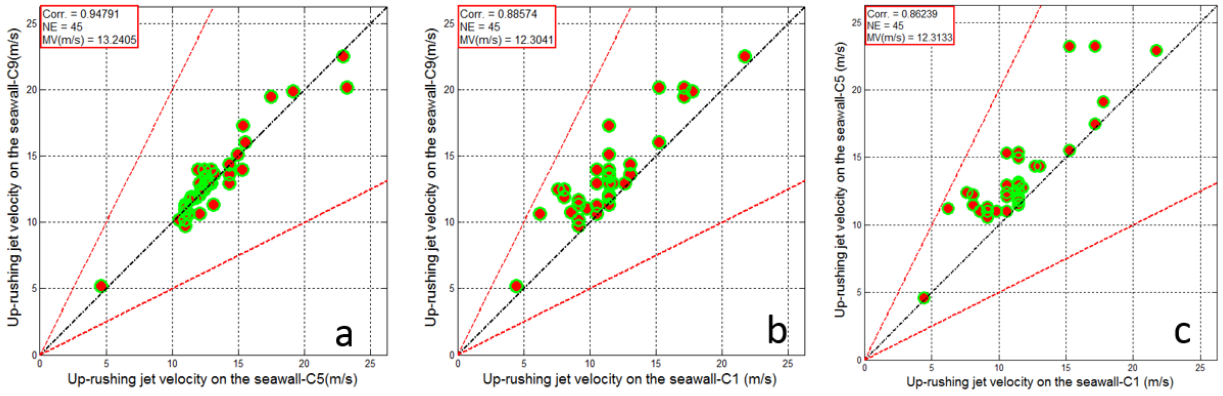

Figure 9. Correlation test for predicted velocities in Figure 8b-d, dash-dotted black line is the perfect correlation line and dashed red lines are the scattering detectors with a factor of two. a) Correlation between C5 and C9; b) correlation between C1 and C9; b) correlation between C1 and C5.

4 Conclusions

A systematic methodology on the basis of an image processing technique to capture the characteristics of up-rushing jets/crests induced by breaking/non-breaking waves was introduced. Its application on large scale tests with a range of regular waves yielded encouraging results. For velocity estimations, the methodology suggested here appears to be both robust and relatively simple to apply but extracting thickness related information is not as straight forward.

5 Acknowledgments

The authors gratefully acknowledge the support of the European Community's 7th Framework Programme through the grant to the budget of the Integrating Activity HYDRALAB IV, Contract no. 261520. The cooperation of FZK staff in design and installation of experimental apparatus is gratefully acknowledged. The last author would also like to acknowledge Dr Gerald Muller's contribution to the development of the idea and the design of the experiments.

6 References

Aagaard, T., Holm, D., 1989. Digitization of wave runup using video records. J. Coast. Res. 5, 547-551.

Allsop, N.W.H., Besley, P., and Madurini, L. 1995. Overtopping performance of vertical walls and composite breakwaters, seawalls and low reflection alternatives, Paper 4.7 in MCS Final Report, *University of Hannover*.

Allsop, N.W.H., Bruce, T., Pearson, J., and Besley,P. 2005. Wave overtopping at vertical and steep seawalls, *Proceedings of the ICE, Maritime Engineering*, 158, 3, 103-114.

Bruce, T., Pearson, J., and Allsop, N.W.H. 2002. Hazards at coast and harbour seawalls-velocities and trajectories of violent overtopping jets, *Proceedings of 28th International Conference on Coastal Engineering*, ASCE, 2216-2226.

Burcharth, H.F., Lykke Andersen, T., Lara, J.L., 2014. Upgrade of coastal defence structures against increased loadings caused by climate change: A first methodological approach. Coastal Eng. 87, 112-121.

Catálan, P.A., Haller, M.C., 2008. Remote sensing of breaking wave phase speeds with application to non-linear depth inversions. Coastal Eng. 55, 93-111.

Franco, L., Gerloni, M. D., and Van der Meer, J.W. 1994. Wave overtopping on vertical and composite breakwaters, *Proceedings of 24th International Conference on Coastal Engineering*, ASCE, 1030-1045.

Stagonas, D., Lara, J. L., Losada, I. J., Higuera, P., Jaime, F. F., Galani, K., Dimas, A., Vousdoukas, M., Kudella, M., and Muller. 2014. Large scale measurements of wave loads and mapping of impact pressure distribution at the underside of wave recurves, *Proceedings of the HYDRALAB IV Joint User Meeting*, 1-10.

Vousdoukas, M.I., Wziatek, D., and Almeida L.P. 2012. Coastal vulnerability assessment based on video wave run-up observations at a meso-tidal, reflective beach. *Ocean Dyn*, 62, 123-137.

Vousdoukas, M.I., Kirupakaramoorthy, T., Oumeraci, H., de la Torre, M., Wübbold, F., Wagner, B., Schimmels, S., 2014. The role of combined laser scanning and video techniques in monitoring wave-by-wave swash zone processes. Coastal Eng. 83, 150-165.

Vousdoukas, M.I., Wziatek, D., Almeida, L.P., 2012a. Coastal vulnerability assessment based on video wave run-up observations at a meso-tidal, reflective beach. Ocean Dyn. 62, 123-137.

Vousdoukas, M.I., Wziatek, D., Almeida, L.P., 2012b. Coastal vulnerability assessment based on video wave run-up observations at a mesotidal, steep-sloped beach. Ocean Dyn. 62, 123-137.

Vousdoukas, M.L., Velegrakis, A.F., Dimou, K., Zervakis, V., Conley, D.C., 2009. Wave run-up observations in microtidal, sediment-starved pocket beaches of the Eastern Mediterranean. Journal of Marine Systems 78, S37-S47.

Wolters, G., Muller, G., Bruce, T., and Obhrai, C. 2005. Large-scale experiments on wave downfall pressures. *Proceedings of the Proceedings of the ICE, Maritime Engineering*, 158, 4, 137-145.